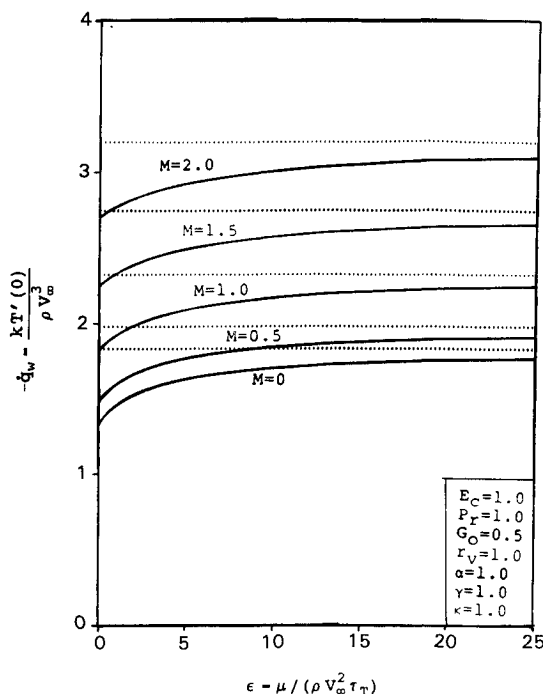


Fig. 1 Fluid-phase temperature profiles.

Fig. 2 Wall heat transfer vs ϵ .

Conclusion

The steady laminar flow solutions of particulates suspended in an electrically conducting fluid past an infinite porous flat plate presented in this article indicate the changes that will be brought about by a transverse magnetic field exhibiting relative motion with the plate. It was found that the heat transfer rate \dot{q}_w increased as the strength of the applied magnetic field increased.

References

- ¹Soo, S. L., "Boundary Layer Motion of a Gas-Solid Suspension," Project Squid Rept. ILL-3P, Univ. of Illinois, Urbana, IL, Oct. 1961.
- ²Marble, F. E., "Dynamics of Dusty Gases," *Annual Review of Fluid Mechanics*, Vol. 2, No. 1, 1970, pp. 297-446.

³Rossow, V. J., "On Flow of Electrically Conducting Fluids over a Flat Plate in the Presence of a Transverse Magnetic Field," NACA TN-3971, May 1957.

⁴Chamkha, A. J., "Exact Solutions for Hydromagnetic Flow of a Particulate Suspension," *AIAA Journal*, Vol. 30, No. 7, 1992, pp. 1922-1924.

⁵Gupta, A. S., "On the Flow of an Electrically Conducting Fluid Near an Accelerated Plate in the Presence of a Magnetic Field," *Journal of the Physical Society of Japan*, Vol. 15, No. 10, 1960, pp. 1894-1897.

⁶Chamkha, A. J., "Convective Heat Transfer of a Particulate Suspension," *Journal of Thermophysics and Heat Transfer*, Vol. 6, No. 3, 1992, pp. 551-553.

Microsensors for High Heat Flux Measurements

J. M. Hager* and L. W. Langley†
Vatell Corporation, Blacksburg, Virginia 24060
 and

S. Onishi‡ and T. E. Diller§
*Virginia Polytechnic Institute and State University,
 Blacksburg, Virginia 24061*

Introduction

MANY different methods have been developed for measuring surface heat flux in aerodynamic flows.¹⁻³ Unfortunately, heat flux gauges are often obtrusive and can cause surface disruptions which result in significant flow disturbances. Even if a smooth surface is maintained, however, the presence of a gauge still usually distorts the temperature field of the surface. This alters the heat flux that the gauge measures and it changes the thermal boundary layer, both of which cause measurement errors.

Figure 1 illustrates a typical heat flux gauge. The heat flux passes through the gauge into the surface and is proportional to the temperature difference $T_1 - T_2$ which is measured by temperature sensors. The temperature at the material surface, however, is different from the temperature at the surface of the gauge, causing the heat flux measured by the gauge to be in error. If an adhesive layer is used for attachment of the gauge to the surface, an additional temperature drop is created. For high-temperature flows the problem is compounded if the gauge is actively cooled. This usually creates a cold spot, which results in an artificially high measurement. As detailed by Neumann et al.⁴ the reliability of the resulting heat transfer measurements is poor.

One way to eliminate the thermal disruption problem is to use passive thin films. When made sufficiently thin, the temperature drop across such a layer becomes negligible, compared to the overall temperature difference between the surface and the fluid. One method that has been used for many years is to infer the heat transfer from thin-film temperature measurements.^{3,5} The heat flux is determined using an analytical model of the transient temperature response of the material. The method is best suited for short-duration flows (~milliseconds), although the test article can also be rapidly injected into a steady flow.⁶

Presented as Paper 91-0165 at the AIAA 29th Aerospace Sciences Meeting, Reno, NV, Jan. 7-10, 1991; received Aug. 2, 1991; revision received May 30, 1992; accepted for publication June 22, 1992. Copyright © 1991 by the American Institute of Aeronautics and Astronautics, Inc. All rights reserved.

*Project Manager.

†President.

‡Assistant Professor, Department of Electrical Engineering.

§Professor, Department of Mechanical Engineering.

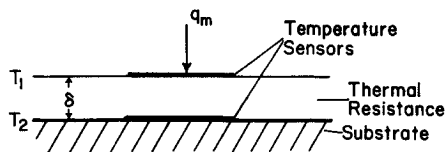


Fig. 1 Layered heat flux gauge.

A different type of thin-film heat flux gauge, called a heat flux microsensor, was first reported by Hager et al.⁷ This is a layered gauge, as illustrated in Fig. 1, consisting of several thin-film layers forming a differential thermopile across a thermal resistance layer. Because the gauge is sputtered directly onto the surface, the total thickness is less than $2\text{ }\mu\text{m}$, which is much less than previous layered gauges. The resulting temperature difference across the thermal resistance layer ($\delta < 1\text{ }\mu\text{m}$) is very small, even at high heat fluxes. To generate a measurable signal, many thermocouple pairs are put in series to form a differential thermopile. The gauge is not only physically nonintrusive to the flow, but also causes minimal disruption of the surface temperature. Because it is so thin, the response time (as reported by Hager et al.⁸) is approximately $20\text{ }\mu\text{s}$. Unlike the transient thin-film gauges, however, the signal of the heat flux microsensor is proportional to the heat flux and gives a continuous measurement. Therefore, it can be used in both steady and transient flows, and measures both the steady and unsteady components of the surface heat flux.

This note describes a new design of the heat flux microsensor which has through-leads and uses high-temperature materials. The goal is to produce a gauge which is capable of high temperature operation. Applications for such a gauge include gas turbine engines, rocket nozzles, combustors, fluidized beds, and hypersonic flow test facilities. Examples are provided of its use in supersonic flows and combusting flames.

New Gauge Design and Fabrication

The new version of the heat flux microsensor was fabricated using stainless steel masking techniques⁸ instead of wet chemical processing. The original etched mask design was a dense layout of 96 thermocouple pairs. Because of the large signals at high heat flux, however, the number of thermocouple pairs could be reduced to 40. The overall layout and size of the previous design⁸ were retained. An overlay pattern of the six different layers of the new design is shown in Fig. 2. The distance between the conductors was increased to reduce the occurrence of short circuits and to allow the use of a pulsed argon laser to generate the stencil masks. A computer-controlled process was developed, whereby, a 0.05-mm -thick stainless steel sheet could be laser cut with good repeatability and accuracy without distortion of the material.

Stainless steel masks are generated for each layer of the sensor. Each mask is fixed to the surface of the substrate allowing the sputtered films to grow only in the areas where the apertures allow the particles through. Subsequent layers are precisely aligned one at a time under a microscope until the six layers of the sensor have been completed. Since the stainless steel masks don't require any substrate chemical processing, such as photoresist, the deposition temperatures could be increased to $300\text{--}400^\circ\text{C}$. Using high substrate temperatures during deposition reduces the internal stresses in the film and increases adhesion.

New thermocouple materials were also investigated to increase the microsensor temperature limits. Nichrome and platinum were chosen because their thermoelectric potential is relatively large and they can withstand continuous temperatures in excess of 500°C .

The new heat flux microsensors were fabricated on 25-mm -diam, 6.25-mm -thick aluminum nitride substrates. Aluminum nitride was chosen as a substrate because of its high thermal conductivity for a ceramic ($140\text{--}170\text{ W/m}\cdot\text{K}$), and because it can be polished to a smooth, flat surface, which makes thin-

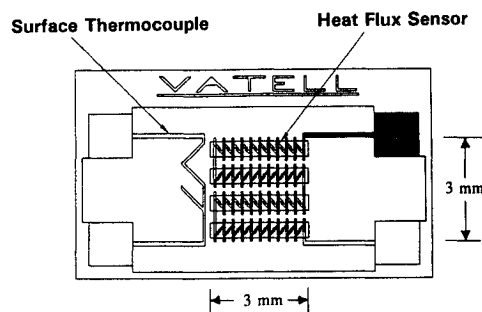


Fig. 2 High-temperature microsensor pattern.

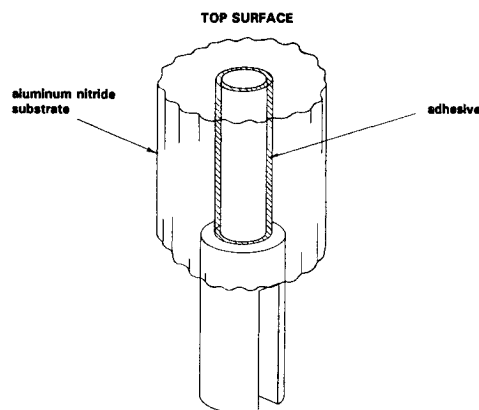


Fig. 3 Through pin connection.

film fabrication easier. Moreover, ceramic substrates eliminate the difficulties involved in isolation of the electric circuits from conducting substrates.

Through-leads provide a means for the sensor signal to be brought through the substrate to instrumentation connections on the backside. They are particularly desirable for aerodynamic testing to minimize surface disruption. The main difficulty is achieving a good ohmic connection between the thin film and the through-lead. The holes in the aluminum nitride substrates were drilled to a diameter of 1.0 mm and were fit with pins having a 0.75-mm diam within the substrate and a 1.75-mm diam behind the substrate, as shown in Fig. 3. The pins were fixed in the substrate using high-temperature alumina cement, and the sensor was fabricated on the surface. The tops of the pins were coated with a thin, smooth layer of silver epoxy at the film connection after all sputtering was completed. The connections survived many harsh tests including supersonic airflow, high-temperature flame tests, and impact surface loads. Connection of the through pins with the instrumentation was done by spot-welding nichrome and platinum wires. These wire pairs were twisted and shielded for 50 cm and connected to a twisted, shielded pair to the instrumentation. This connection was sufficiently far from the test apparatus to assure that additional thermoelectric potentials were not created.

Heat Flux Calibration

Because the heat flux microsensors were designed to measure convective heat transfer, the sensors were calibrated in convection. In previous work, the sensor was mounted in a heated plate for steady-state calibrations.⁸ To achieve higher heat fluxes, a transient calibration was used in the present work. This is possible because the sensor measures both heat flux and surface temperature simultaneously, and the response time is much faster than the transient.

The sensor was mounted at the center of a heated aluminum plate. A 1.6-cm free jet was directed normal to the sensor surface from a distance of 7.6 cm . The jet was shuttered onto the sensor after the set-point temperature of the plate was

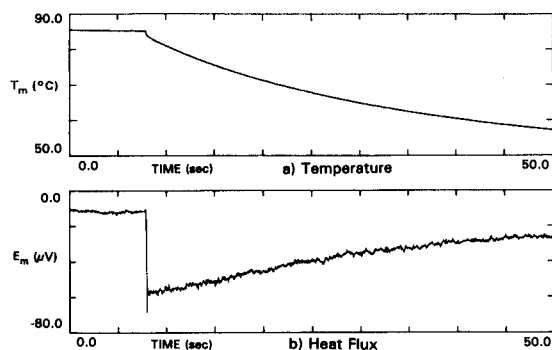


Fig. 4 Transient calibration.

reached, resulting in a step change in the heat flux signal from the sensor. Both the temperature signal from the surface thermocouple and the heat flux signal were simultaneously recorded on an HP digital signal analyzer for up to 1 min, as shown in Fig. 4. The magnitude of the heat flux signal, E_m , decreases as the temperature difference between the sensor, T_m , and the air, T_a , decreases, due to the cooling of the substrate, as shown in the upper temperature trace. The heat transfer coefficient for this flow configuration had previously been measured using a calibrated Gardon gauge⁹ as $h = 200 \text{ W/m}^2 \cdot \text{K}$ (estimated uncertainty of $\pm 7.5\%$). The heat flux q_m was calculated from the heat transfer coefficient and the instantaneous surface and airflow temperatures as

$$q_m = h(T_a - T_m) \quad (1)$$

Matching this with the microsensor output, E_m , gives the gauge sensitivity at any point in time:

$$S = (E_m/q_m) \quad (2)$$

The gauge sensitivity was constant over most of the range measured, $S = 15.5 \mu\text{V}/(\text{W}/\text{cm}^2)$. The total estimated uncertainty for the sensitivity is $\pm 10\%$ with this calibration. Although less uncertainty is often quoted for radiation calibration methods, the convection calibration is more representative of the ensuing test conditions. A comparison of these two methods is reported by Terrell et al.¹⁰

The surface thermocouple was calibrated in place in the same apparatus. A 0.075-mm type-T thermocouple was attached to the face of the substrate next to the surface thermocouple. A thick piece of insulation was placed over the entire surface of the plate to perform soak-temperature measurements. Monitoring both the output of the surface thermocouple, referenced to ice-point, and the type-T thermocouple for various steady-state heater settings, a calibration over the apparatus temperature range was performed giving $13.9 \mu\text{V}/^\circ\text{C}$.

Microsensor Measurements

The measurement capabilities of the heat flux microsensor were demonstrated for two applications. The gauge was first mounted flush in the wall of a supersonic wind tunnel. This is a blow-down system with atmospheric total pressure and temperature. Consequently, the recovery temperature of the Mach 2.4 flow, once established, was lower than ambient. The resulting heat flux from the wall is shown on the time trace of Fig. 5a as a negative sensor signal. The heat flux is directly proportional to the sensor signal

$$q_m = (E_m/S) \quad (3)$$

with an estimated repeatability uncertainty of $\pm 0.05 \text{ W}/\text{cm}^2$. The effect of the starting shock on the heat transfer is also clearly seen on the trace. The heat transfer into the wall is positive as the front of the shock passes and negative behind it. A simultaneous static pressure trace was taken by a pres-

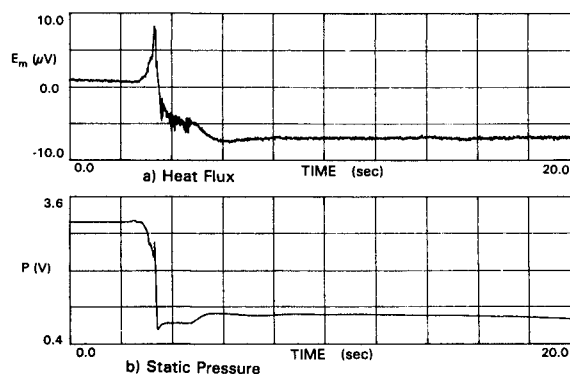


Fig. 5 Supersonic wind-tunnel test.

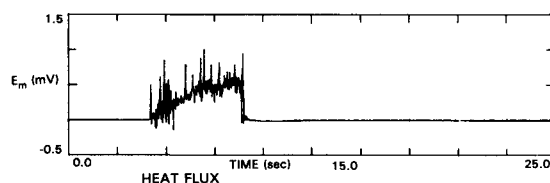


Fig. 6 Propane flame test.

sure transducer mounted flush in the tunnel wall. The starting transients can easily be matched from the corresponding heat flux and pressure time traces in Fig. 5. This test demonstrates some of the desirable characteristics of the gauge. Because it is a passive gauge, it measures heat flux both to and from the wall. Its fast time response captures the effects of shock passage over the gauge, but the continuous output can be recorded over the entire 20-s time trace.

The heat flux microsensor was fabricated out of materials capable of withstanding high temperatures. The melting points of nichrome and platinum, the primary materials of the sensor, are 1769°C and 1350°C , respectively. However, the adhesion of these materials as thin films on aluminum nitride is not expected to withstand such extreme temperatures. Tests were performed to determine at what temperature the thin films would lose adhesion, uncoated and coated with a ceramic layer. The platinum did not show signs of adhesion loss after being heated over a long period to 1100°C . The uncoated nichrome severely oxidized by 500°C , yet survived to at least 700°C when coated.

For a high-heat flux test, a small chimney was built around a Bunsen burner and a water-cooled fixture for the sensor was mounted at the top. Propane was used for the fuel because it produces flame temperatures of 1200 – 1900°C . The top of the chimney protected all but the face of the disk from the open flame. Cold tap water was circulated through the aluminum block fixture to help keep the disk cool and maintain a high heat flux level. The flame temperature close to the front of the sensor was monitored by a type-K wire thermocouple. The flame was adjusted to fully engulf the sensor for approximately 4–10 s, or until the wire thermocouple measured at least 1000°C . Figure 6 shows that the measured heat flux [from Eq. (3)] reached $30 \text{ W}/\text{cm}^2$ during a typical test with a large component of unsteadiness in the heat flux. The sensor withstood as many as 30 such tests until failure occurred. The thin-film thermocouple was not intact for these tests, so traces of the gauge surface temperature were not recorded. Subsequent tests have indicated that the surface temperature did not exceed 100°C .

Conclusions

A new heat flux gauge has been designed and tested. A successful through-lead technique has been developed. The resulting gauge was used extensively for measurements in supersonic flow and in propane flames. The effects of shock passage were clearly seen in supersonic flow, demonstrating the gauge's measurement capability of transient events. The

flame measurements demonstrated survivability and measurement capability in high heat flux environments.

Acknowledgments

This work was supported by the National Science Foundation under Grant CBT-8814364. The Government has certain rights in this material. The authors also acknowledge the cooperation of the Hybrid Microelectronics Laboratory of Virginia Polytechnic Institute and State University.

References

- ¹Neumann, R. D., "Aerothermodynamic Instrumentation," AGARD Rept. 761, 1989.
- ²Diller, T. E., and Telonis, D. P., "Time-Resolved Heat Transfer and Skin Friction Measurements in Unsteady Flow," *Advances in Fluid Mechanics Measurements, Lecture Notes in Engineering*, edited by M. Gad-el-Hak, Springer-Verlag, Berlin, 1989, pp. 323–355.
- ³Oldfield, M. L. G., "Experimental Techniques in Unsteady Flows," *Unsteady Aerodynamics*, Vol. 1, von Karman Inst. for Fluid Dynamics, Rhode Saint Genese, Belgium, 1988.
- ⁴Neumann, R. D., Erbland, P. J., and Kretz, L. D., "Instrumentation of Hypersonic Structures—A Review of Past Applications and Needs for the Future," AIAA Paper 88–2612, June 1988.
- ⁵Jones, T. V., "Heat Transfer, Skin Friction, Total Temperature, and Concentration Measurements," *Measurement of Unsteady Fluid Dynamic Phenomena*, Hemisphere, New York, 1977, pp. 63–102.
- ⁶O'Brien, J. E., "A Technique for Measurement of Instantaneous Heat Transfer in Steady-Flow Ambient-Temperature Facilities," *Experimental Thermal and Fluid Science*, Vol. 3, No. 4, 1990, pp. 416–430.
- ⁷Hager, J. M., Onishi, S., Langley, L. W., and Diller, T. E., "Heat Flux Microsensors," *Heat Transfer Measurements, Analysis and Flow Visualization*, edited by R. K. Shah, American Society of Mechanical Engineers, 1989, pp. 1–8.
- ⁸Hager, J. M., Simmons, S., Smith, D., Onishi, S., Langley, L. W., and Diller, T. E., "Experimental Performance of a Heat Flux Microsensor," *Journal of Engineering for Gas Turbines and Power*, Vol. 113, No. 2, 1991, pp. 246–250.
- ⁹Borell, G. J., and Diller, T. E., "A Convection Calibration Method for Local Heat Flux Gages," *Journal of Heat Transfer*, Vol. 109, No. 1, 1987, pp. 83–89.
- ¹⁰Terrell, J. P., Hager, J. M., Onishi, S., and Diller, T. E., "Heat Flux Microsensor Measurements and Calibrations," NASA CP3161, April 1992, pp. 69–80.

Thermally Developing Convection from Newtonian Flow in Rectangular Ducts with Uniform Heating

B. T. F. Chung,* Z. J. Zhang,† and G. Li‡

University of Akron, Akron, Ohio 44325

and

L. T. Yeh§

Texas Instruments, Inc., Dallas, Texas 75286

Introduction

THE fluid flow and heat transfer behavior of laminar flow through rectangular ducts is of special interest because

Received March 6, 1992; revision received July 9, 1992; accepted for publication July 14, 1992. Copyright © 1992 by the authors. Published by the American Institute of Aeronautics and Astronautics, Inc., with permission.

*Professor, Department of Mechanical Engineering.

†Graduate Student, Department of Mechanical Engineering.

‡Graduate Student; currently Design Engineer, ABB Garden City Fan, Niles, Michigan 49120.

§Currently Senior Engineering Specialist, Loral Vought Systems, Dallas, Texas 75265.

of the wide application of such a geometry in compact heat exchangers. Consequently, extensive studies have been carried out on such a geometry. An excellent comprehensive review of laminar flow forced convection in duct was presented by Shah and London.¹ Recently, Hartnett and Kostic² gave an up-to-date collection of literature in the heat transfer aspect for rectangular duct flows. The boundary conditions referred to by these authors fall into the three categories: 1) constant wall temperature both peripherally and axially, known as *T* boundary condition; 2) constant heat input per unit axial distance and constant peripheral wall temperature at each axial position with wall temperature varying axially only, referred to as *H1* boundary condition; and 3) constant heat input per unit axial distance as well as per unit peripheral distance, this is denoted by *H2* boundary condition.

Clark and Kays³ and Schmidt and Newell⁴ numerically evaluated the Nusselt number for rectangular ducts under both *T* and *H1* boundary conditions. Sparrow and Siegel⁵ developed a variational approach for heat transfer in rectangular ducts for the *H2* boundary condition. All these studies are limited to the hydrodynamically and thermally fully developed condition.

A few investigators considered the case of hydrodynamically fully developed and thermally developing Newtonian flow. Montgomery and Wibulswas⁶ used a finite-difference method to solve for the Nusselt number for rectangular duct for *T* and *H1* boundary conditions. Chandrupatla and Sastri⁷ obtained the developing Nusselt numbers under the *T*, *H1*, and *H2* boundary conditions, but only for the square duct geometry.

Our literature survey reveals that there is a lack of general information and treatment on thermally developing laminar flow in rectangular duct for the *H2* boundary condition. Complementary to previous studies, this work is to investigate the behavior of hydrodynamically fully developed and thermally developing laminar flow of Newtonian fluids in rectangular ducts for the *H2* boundary condition.

Analysis

Consideration is given to the system in which a Newtonian fluid flows in a horizontal rectangular channel with an arbitrary aspect ratio subject to *H2* boundary condition. Let the origin of the coordinates be set at a lower corner of the duct; the axial direction along which the fluid flows coincides with the *z* axis and the cross section area of the duct, $2a \times 2b$ is perpendicular to the *z* axis. The present analysis is based on the following assumptions: 1) hydrodynamically fully developed laminar flow of Newtonian fluids, 2) steady-state, 3) constant fluid properties, and 4) neglecting axial conduction and viscous dissipation.

The momentum equation of Newtonian fluid takes the form of

$$\frac{\partial^2 w}{\partial x^2} + \frac{\partial^2 w}{\partial y^2} = \frac{1}{\mu} \frac{dp}{dz} = \text{const} \quad (1)$$

Equation (1) is solved analytically by the separation of variables. The final solution is

$$w = \frac{g_c}{2\mu} \frac{dp}{dz} a^2 \left\{ \frac{32}{\pi^3} \sum_{n=1,3,5,\dots}^{\infty} \frac{1}{n^3} (-1)^{(n-1)/2} \cdot \cos \left[\frac{n\pi(x-a)}{2a} \right] \frac{\cosh(n\pi(y-b)/2a)}{\cosh(n\pi b/2a)} - \left[1 - \left(\frac{x-a}{a} \right)^2 \right] \right\} \quad (2)$$